0.1 Nonlinear tensor wave propagation modeling

ABSTRACT

The interaction of a seismic source device with the free surface of the earth makes the radiation characteristic different from that of the equivalent body point source. Usual seismic sources are built to produce enough energy to penetrate a few kilometers into the earth. There is no guarantee that when the source is activated, the surface material behavior will stay within a region that can be appropriately described using infinitesimal stress strain relationships. In this section I use finite-differences to model radiation characteristics and wave propagation when the equations of motion are no longer linear. I extend a nonlinear scalar equation that is normally used in one dimension into a three component, three-dimensional setting.

0.1.1 Nonlinearities in a seismic experiment

When a time dependent forcing function is generated, nonlinear behavior can occur in the electronic amplification part of the system. These nonlinearities can be avoided by the use of feedback mechanisms (**?**). Another nonlinear mechanism is the transfer of the desired signal into the ground. Most of the signal distortion occurs at this instance with high momentum devices by impact or vibration. The subsurface volume in which such mechanisms dominate is rather small, yet such nonlinear behavior shows up as an effective alteration of the signal spectrum and depends on radiation direction. It is this interaction of the device with the earth's surface that cannot be described adequately by the use of infinitesimal displacements or stresses. When one describes nonlinearities two effects come into play: the finiteness of the variables and the possibility of entering a nonlinear region in the stress-strain relationship. In general, the function describing the stress-strain dependency, (cf. Figure 0.1) may be arbitrary as long as some underlying conservation principles (energy, momentum) are satisfied. It is always possible to expand this function around an equilibrium point. A conventional elastic method would only use the linear term of such a Taylor series expansion. This works well if the magnitude of the variables is small. If the magnitude exceeds a certain limit, one has to use higher order terms in the approximation to describe the medium accurately. It is seldom the case that these higher order stiffness constants are measured. For this reason, this section mainly deals with effects introduced by the finiteness of the variables, but not with the nonlinear stress-strain relationship. Fortunately, the finiteness of displacements introduces no new material parameters that must be known or estimated. Allowing the displacements to be non-infinitesimal merely means that the volume is deformed by finite displacements. This is equivalent to allowing higher order terms in the Taylor expansion of

the displacement field. This section does not deal with receiver properties, although the same framework can be applied to modeling and estimating receiver functions. I assume that receiver properties can be effectively described using their transfer function. Most of the external effects are likely to be caused by ground coupling. Stresses and displacements at receivers are generally many orders of magnitudes smaller than at sources.

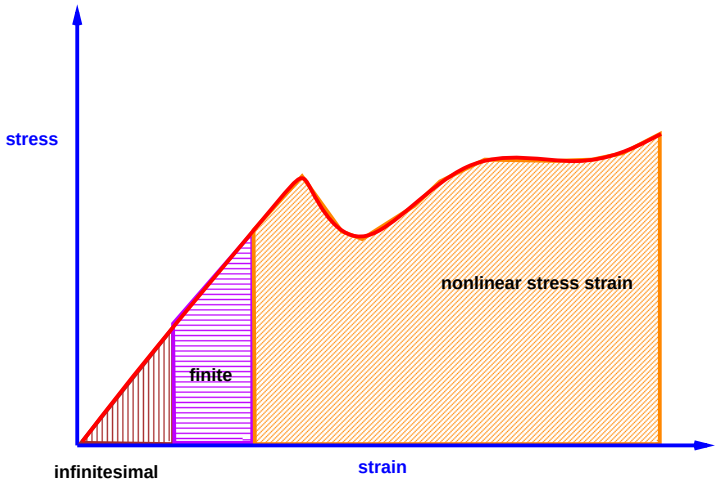

Figure 0.1: Stress-strain relationships can be arbitrary, as long as some underlying conservation principle holds. The region of infinitesimal strain is at around 10^{-6}, while the geometric nonlinearity allows strain in the magnitude of 10^{-3}. Above that value the stress-strain relationship enters the nonlinear-medium region. stress-strain [NR]

0.1.2 Abandoning linearity

Geometric nonlinearity

If the deformation is less than 10^{-3} (?) in an elastic region (cf. Figure 0.1), nonlinearity is assumed to result from finite geometry and not from a nonlinear stress-strain relation. However, the line between geometric and material nonlinearity cannot be drawn clearly. Following Biot (?), it is possible to compute the material deformation to second order as

$$\epsilon_{kl} = e_{kl} + 1/2(e_{k\mu}\omega_{\mu l} + e_{l\mu}\omega_{\mu k}) + 1/2(\omega_{k\mu}\omega_{l\mu}) \tag{0.1}$$

$$e_{kl} = 1/2(\frac{\partial u_k}{\partial l} + \frac{\partial u_l}{\partial k}) \qquad \text{and} \qquad \omega_{kl} = 1/2(\frac{\partial u_k}{\partial l} - \frac{\partial u_l}{\partial k}) \quad . \tag{0.2}$$

Neglecting the rotational tensor components ω in (0.1) results in the usual definition of the elastic symmetric strain tensor e. Following Fung (?), we have a similar formulation for the Eulerian strain tensor:

$$\epsilon^E_{kl} = 1/2(\frac{\partial u_k}{\partial l} + \frac{\partial u_l}{\partial k}) - \frac{\partial u_m}{\partial k}\frac{\partial u_m}{\partial l} \quad . \tag{0.3}$$

Both equation (0.1) and (0.3) describe the deformation of a medium to a higher order than the usual elastic strain tensor e. The deformation in Figure 0.2 is a pure

geometrical property and not a material property. Consequently, the linear Hooke's law

$$\sigma_{ij} \;=\; b_{ijkl} \;\; \epsilon_{kl} \tag{0.4}$$

remains unmodified. The relation between stress and strain components is still linear. It is the computation of ϵ_{kl} that changes in each case. When considering the displacement gradients, we can see that higher order gradient components are related to stress components nonlinearly. However, the parameters which link them, the stiffness coefficients b_{ijkl}, are still linear elastic parameters. All previous equations lead to an elastic wave equation of the form

$$\nabla \underset{\sim}{\mathbf{b}} \nabla^t \, \mathbf{u} - \rho \frac{\partial^2 \mathbf{u}}{\partial t^2} = \mathbf{f} \; , \tag{0.5}$$

or, in the geometrically nonlinear case, to a slight modification of the previous expression:

$$\nabla_g \underset{\sim}{\mathbf{b}} \nabla_g^t \, \mathbf{u} - \rho \frac{\partial^2 \mathbf{u}}{\partial t^2} = \mathbf{f} \; , \tag{0.6}$$

where ∇_g is the geometrically nonlinear derivative operator.

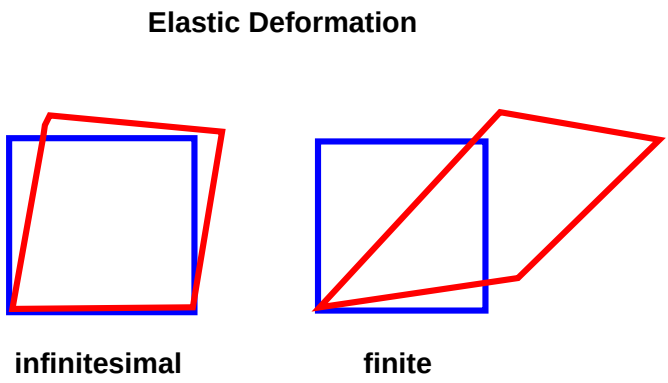

Figure 0.2: Finite elastic deformation is a purely geometric effect. The strain does not yet enter the region where the medium itself behaves nonlinearly. Stress and strain components are still related through a linear relationship. finite [NR]

Material nonlinearity

The next higher level of complexity involves the use of nonlinear relations between stress and strain components. Even when displacement gradients are computed to first order, only the higher order material relationship introduces higher order effects in the differential equation. Material nonlinearity might easily be coupled with geometric nonlinearity; drawing a clear boundary between them might be hard in many cases. This kind of nonlinearity introduces new parameters into the differential equation, namely, new material constants (higher order elastic parameters). In many practical cases one might not have knowledge of these parameters, or they might be hard to estimate.

Omission of the second and higher order cross terms ensures that a wave equation is linear. If these terms are neglected in the Taylor expansion of $d\mathbf{u}$, one is still

confined to examining only a small neighborhood around a reference point. The assumption that the products of the displacement gradients are small assures that the principle of superposition remains valid.

One needs to use equations (0.1) and (0.3) as soon as one considers finite displacements of the medium. It is practical to start with such a nonlinear description since it introduces only small modifications of existing modeling programs, while admitting some degree of nonlinearity. Since algorithms that are based on linear assumptions fail in this case, other methods have to be used to solve the problem. The wave equation, therefore, will be nonlinear in the spatial domain; in the time domain, the principle of superposition is still valid. In order to investigate the impact of nonlinearity on radiation patterns and signal wave forms, one can calculate numerical examples in which nonlinear wave propagation is modeled using finite differences in time and space. Such a model should serve as a lower limit of what we can expect from nonlinearities.

0.1.3 Modeling with finite-differences

Many geophysical numerical algorithms assume linearity. Thus, they will work only on equations that have a linear behavior. For modeling nonlinear phenomena, the choice of algorithms becomes rather restrictive. In most cases, an analytical solution is not possible or would involve some sort of linearization. That, in turn, would defeat the original purpose of investigating nonlinear effects. For modeling nonlinearities finite difference algorithms have the advantage of not having to make linearity assumptions in order to model nonlinear wave propagation. However, one problem with the use of finite difference methods remains: it is now much harder to calculate stability criteria properly, since many rigorous stability criteria are based on linearity. The usual methods use linear transforms to produce an easily calculated estimate of stability and dispersion of the algorithm. In a recent paper Kosik (**?**) makes use of a Crank-Nicholson FD scheme that is implicit and is thus guaranteed to exhibit stability for a certain range of parameters, but how much such an implicit method averages out nonlinear effects is debatable.

Applicability

For investigating surface source behavior, the previously described notion of finite stresses and strains in a medium can be readily applied to surface source of different types. Multi-component impulsive or vibratory sources could generate a region in the subsurface in which such nonlinear behavior is appropriate. However, such a region, as shown in Figure 0.3, might be relatively small compared to the source wavelength. For data processing, a far-field description with an effective source is more efficient. It allows a different parameterization of source behavior that depends on the experiment type and the data itself. However, when modeling source behavior for the purpose of testing source equalization schemes, such as those described in chapter **??**,

it is valuable to have numerical algorithms that allow modeling of nonlinear source behavior.

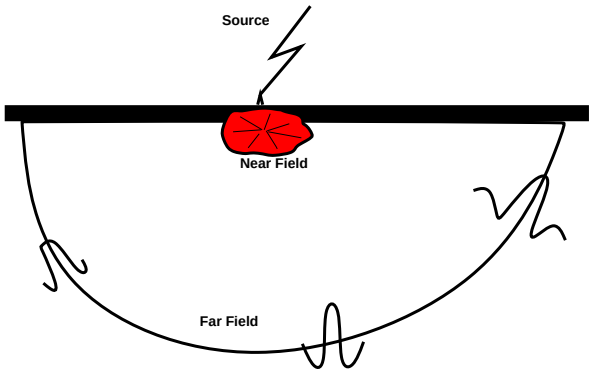

Figure 0.3: Nonlinear near-field source behavior generates far-field effects, such as amplitude variations and wavelet frequency content that can vary with angle. For seismic data processing an effective far-field source behavior has to be determined. region [NR]

0.1.4 Chaotic sources

The above paragraph describes the nonlinear source behavior of an elastic medium that obeys the "usual elastic" anisotropic wave equation. However, an investigation by Walker (**?**) shows that the time dependence of source-surface interactions of vibrators can be effectively described using a nonlinear "chaotic" wave equation. Walker uses the well-known Duffing equation to parameterize vibratory sources and nonlinear propagation in the subsurface. The one dimensional Duffing equation is given as

$$\alpha u + \frac{\partial^2 u}{\partial t^2} + \delta \frac{\partial u}{\partial t} + \gamma u^2 + \beta u^3 = F \cos(\omega t) \quad , \tag{0.7}$$

where α, β, γ and δ are adjustable parameters that govern the nonlinear behavior, u is a scalar quantity, F is the strength of the periodic forcing function, and ω the temporal frequency.

The time dependent solution $u(t)$ of the Duffing equation exhibits typical behavior for a wide range of parameters. When the source-surface system is at a high energy level, the amplitudes are large. Harmonics that alter the high frequency part of the spectrum of the original source wavelet are then generated. When the amplitudes are low, the nonlinear behavior creates subharmonics that introduce low frequency peaks. Such a period-doubling phenomenon is typical of chaotic equations. The typical chaotic behavior, however, occurs in band-limited intervals of the forcing function's spectrum. Outside those intervals, the equation behaves pseudo-regularly. The following figures show some of that behavior. Unless otherwise noted, the parameters are set to zero. In practice, only a of the effects that are possible, are indeed observed with surface seismic data: top- and sub-harmonics, as illustrated in the third and fourth plot from the top in Figure 0.4. The top plot in Figure 0.4 shows a constantly growing signal, resulting from a system that is not damped or limited in any way. The second

plot from the top shows a damped linear system. The phase space (displacement plotted versus velocity) is a spiral approaching a constant orbit. The time domain response is well behaved and the spectrum shows a single peak developed around the center frequency of the forcing function. Some harmonic peaks, in the third plot from the top, are generated in the spectrum beyond the peak of the forcing function. High amplitudes arise by means of an emphasis on the third order term in the equation. As the fourth plot in Figure 0.4 illustrates, subharmonic peaks are generated in the spectrum below the peak of the forcing function. Relatively low amplitudes are generated here, in contrast to the amplitudes for topharmonics. Nonlinear behavior has developed in the signal response (shown in the fifth plot from the top in Figure 0.4) at this parameter setting and the signal is apparently erratic in the phase space. The spectrum of the forcing function is changed in a non-systematic way. Compare this to the structured modifications that generate subharmonics and topharmonics. The last two plots in Figure 0.4 show slightly different parameter settings and illustrate the unstable character of this equation. Small changes in parameters produce large effects in the solution behavior.

0.1.5 Duffing extended for three components and three dimensions

The original Duffing equation describes a scalar chaotic process and has been used in the past to model and to analyze the effective time behavior of a source-surface system. I extend the scalar equation and use it for multi-component sources in an anisotropic 3-D medium. Equation (0.7) is a harmonic oscillator equation with additional nonlinear terms added. I construct a similar equation for the case in which the wave field is of vectorial nature and extends in three dimensions. Starting with the general elastic wave equation (**??**), the first two terms in (0.8) correspond to the harmonic oscillator analog of equation (0.7).

$$\nabla \underset{\sim}{\mathbf{b}} \nabla^t \mathbf{u} - \rho \frac{\partial^2 \mathbf{u}}{\partial t^2} + \nabla \underset{\sim}{\mathbf{c}} \nabla \frac{\partial \mathbf{u}}{\partial t} + \underset{\sim}{\gamma} ||\mathbf{u}||^2 + \underset{\sim}{\beta} \mathbf{u} ||\mathbf{u}||^2 = \mathbf{F}(\mathbf{x}, t) \tag{0.8}$$

I extended the terms to allow for three space dimensions and tensorial stress and strain quantities instead of a one-dimensional displacement; thus I also allow for fully anisotropic behavior. The third term $\nabla \underset{\sim}{\mathbf{c}} \nabla \frac{\partial \mathbf{u}}{\partial t}$ adds a viscous damping factor; in equation (0.7) this is only a scalar parameter, while in equation (0.8) it becomes a matrix of viscous moduli. The fourth term, $\underset{\sim}{\gamma} ||\mathbf{u}||^2$, augments the equation by a force that is proportional to the squared magnitude of the displacement. In both equations the total displacement governs the influence of this term. In equation (0.8) the parameters can be of tensorial nature, affecting each displacement vector component differently compared to the original equation (0.7). The fifth and last term, $\underset{\sim}{\beta} \mathbf{u} ||\mathbf{u}||^2$, adds an additional force to the equation that is proportional to the third power of the displacement components. This is similar to a hard spring force taking effect when amplitudes become large, because of the parameters' tensorial

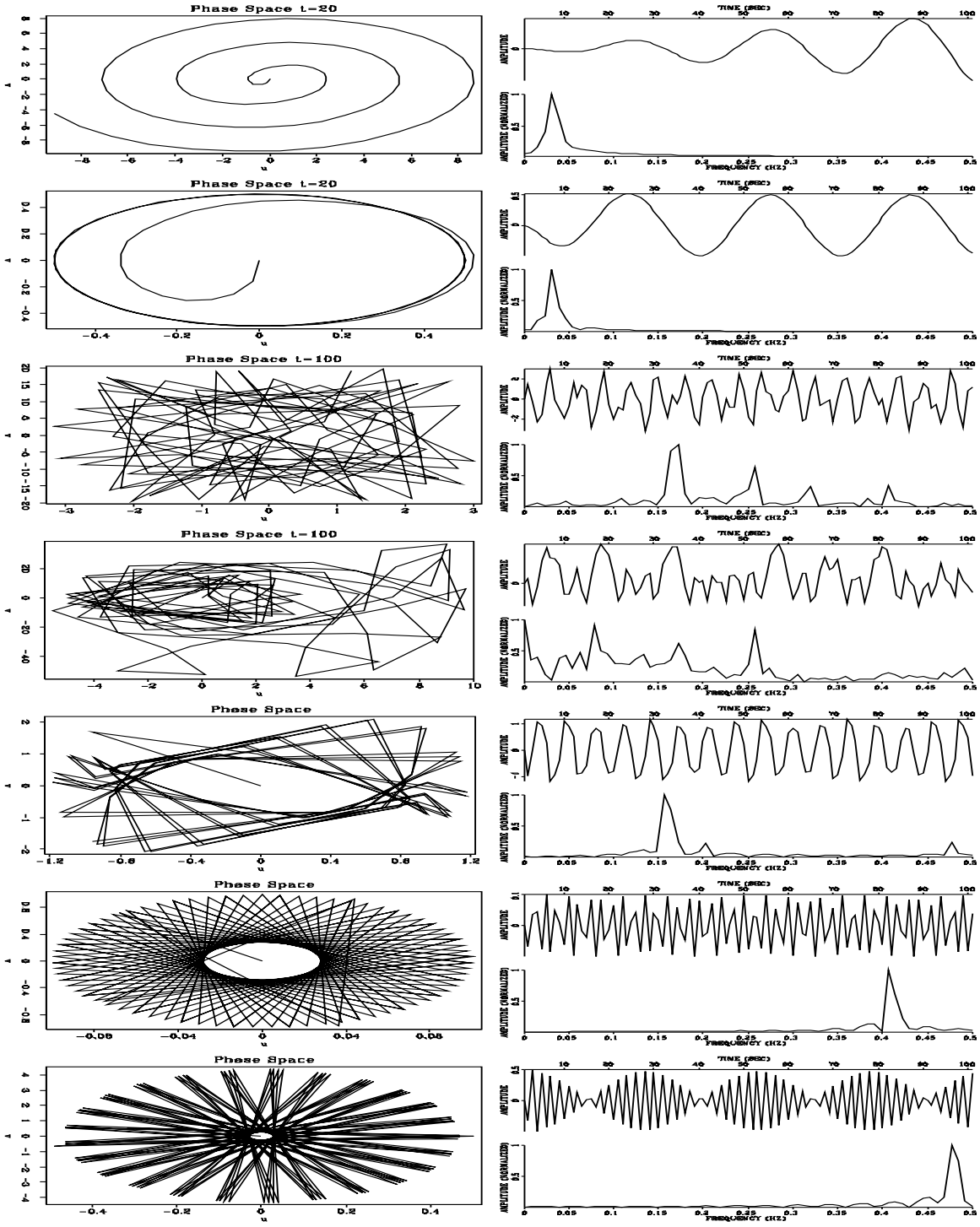

Figure 0.4: Different parameter settings result in completely different behavior of the equation. Phase space plots are on the left and signal and spectral representations are on the right. For seismic waves, generated under realistic conditions by vibrators, only the third to fifth plot (top-harmonics, subharmonics and stable) from the top are significant. chaos [CR]

nature, each of the tensor components can be affected differently. It seems that there are many additional parameters that one needs to know in order to use this equation, but one can restrict the number of unknown parameters by limiting $\underset{\sim}{\gamma}$ and $\underset{\sim}{\beta}$ to being scalars or tensors that have the same relative tensor component magnitude as the elastic stiffness tensor.

In Figure 0.5 and 0.6 I modeled 2D wave propagation using equation (0.8) in a homogeneous isotropic medium to highlight some effects. All the plots consist of sections cut through a fully modeled z-component wave field cube. Each section corresponds to a different face of the cube. The cube has three axes: distance, depth and, propagation time. The front panels show a wave field snapshot taken at about 0.755 seconds propagation time. The top panels correspond to seismograms recorded at the surface. The side panels display the recordings in a bore hole that is located at a 2.8 km distance. In all of the experiments shonw, the source was an identical vertical force acting in about 0.4 km depth. Since the top surface of the model simulated a free surface boundary condition, the upward propagating wave field reflects and follows the primary wave front down into depth with its converted waves.

The top plot in Figure 0.5 shows the propagation of a wave front using a pure visco-elastic medium. In other words, medium parameters $\underset{\sim}{\gamma}$ and $\underset{\sim}{\beta}$ are zero while parameter $\underset{\sim}{\mathbf{c}}$ is given as a small fraction of the elastic moduli $\underset{\sim}{\mathbf{b}}$. The wave field shows a lower frequency content than the purely elastic modeling in the bottom plot. The primary function of the viscosity terms is to disperse the wave field and to damp off high frequencies as propagation continues. In the top plot of Figure 0.6 I activated all the terms in equation (0.8). I compared the higher-order modeling equation to visco-elastic modeling and the difference is a low frequency distortion of the wave field. It shows the strongest effect where the amplitudes in the visco-elastic modeling are high. This is in agreement with the analytical prediction, as the additional forces only depend on the magnitude of the displacement components and thus only indirectly on the medium. A very low frequency tail is visible around the source location. The source component was strongest in the vertical direction at that location and this has a far-reaching effect on the wave field. It is the interplay of a hard spring force and the magnitude force that interacts with the near-source region as long as amplitudes are high. In the bottom plot of Figure 0.6 I model propagation with one of the higher-order terms turned on while the other one is turned off. To better compare the wave fields, I compute the difference of the two displacement fields. The biggest differences are around the high amplitude portions of the wave field; but low-frequency broad-range differences also appear at low amplitudes in the form of expanding circular wave fronts.

0.1.6 Summary

When extending linear wave propagation to a nonlinear regime one can start with a purely geometric parameterization to enter the region of finite stresses and stains: this is a first step that has the advantage of requiring no knowlegde of new material

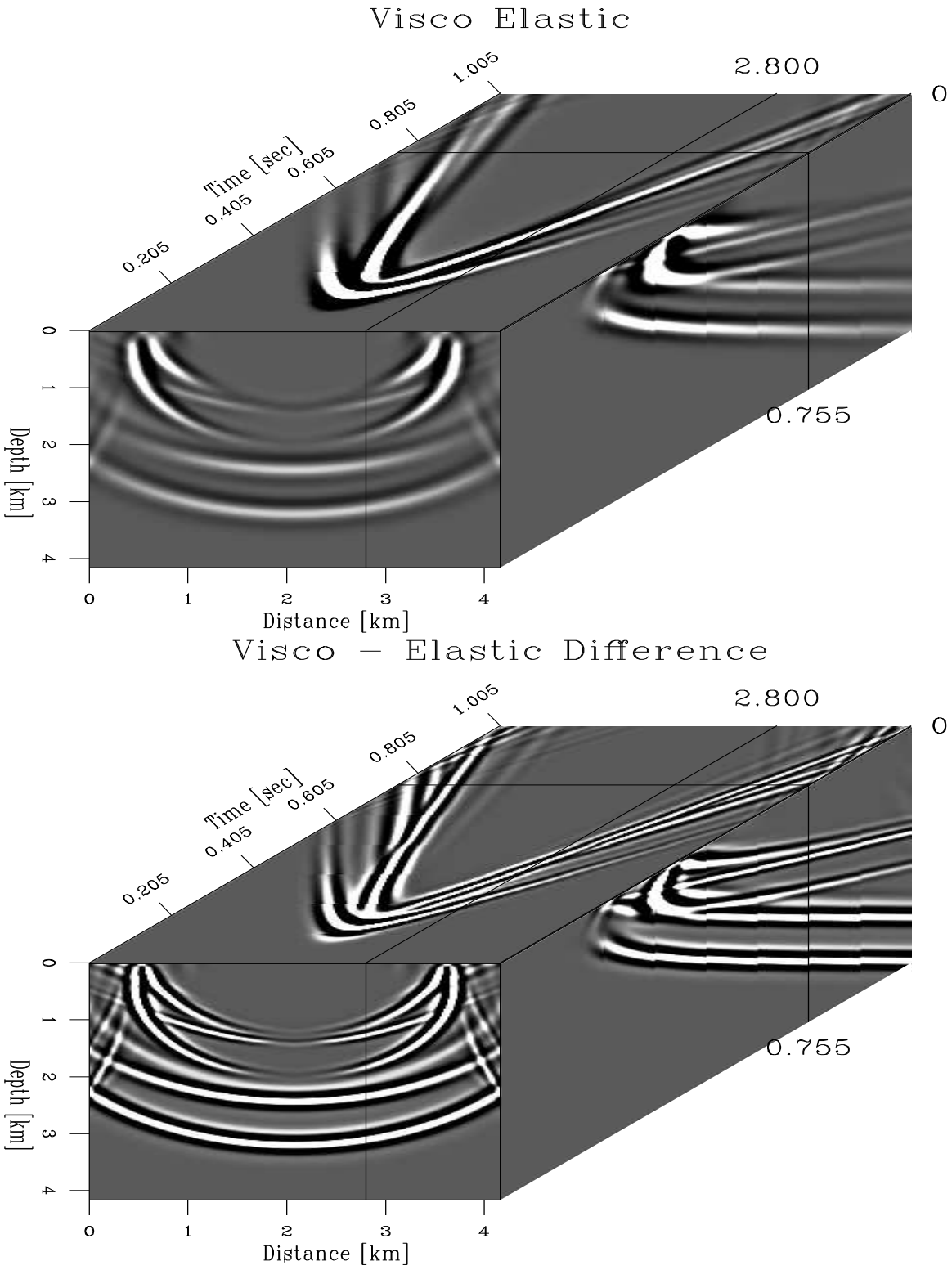

Figure 0.5: The top shows the visco-elastic modeling. The bottom shows the difference between elastic and visco-elastic modeling. elvis [CR]

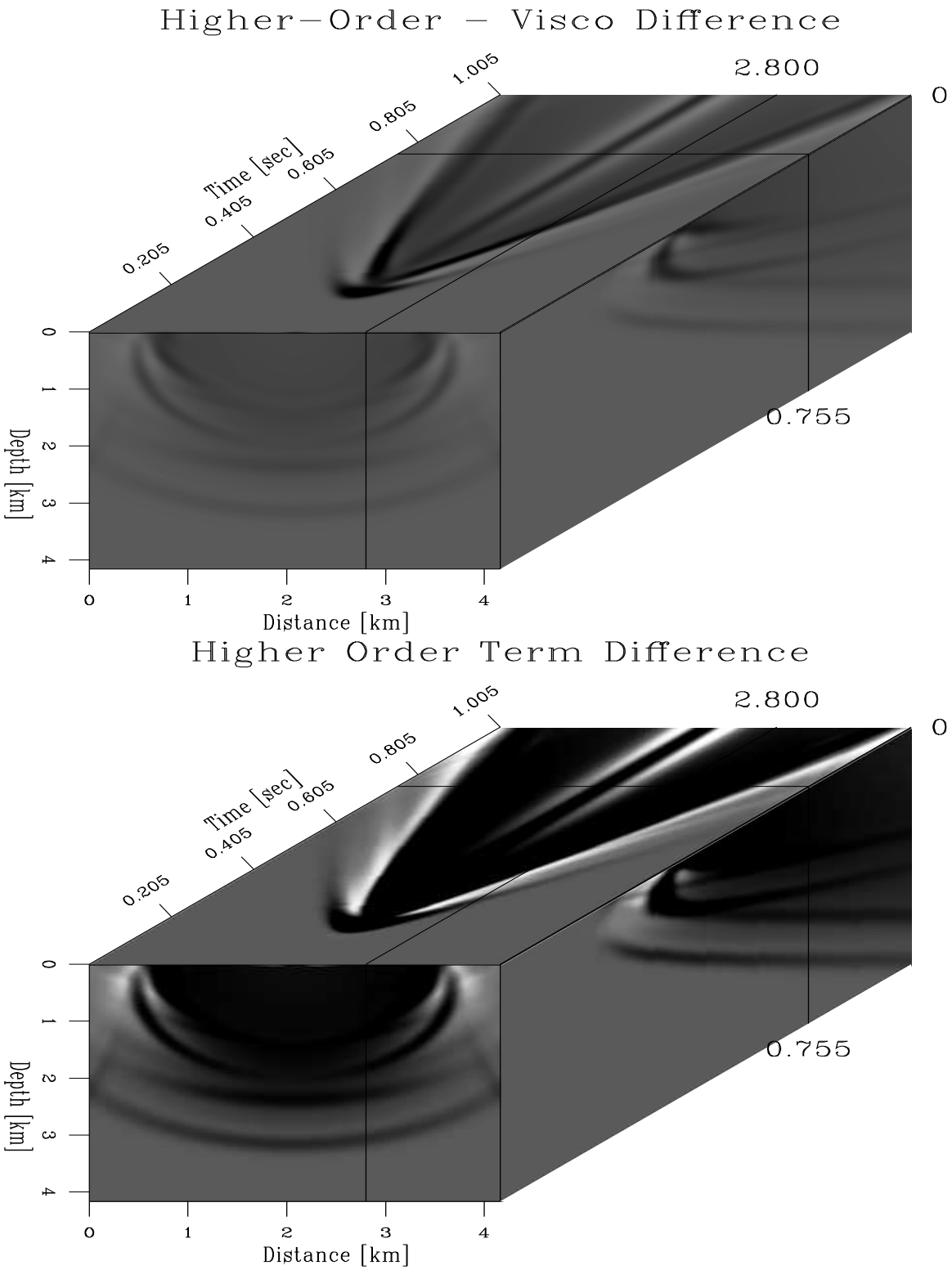

Figure 0.6: The top shows the difference between visco-elastic modeling and modeling with equation (0.8). The bottom shows differences caused only by alternately switching on one higher order term. diffvisduff3 [CR]

parameters. I extend the one-dimensional Duffing equation to three-component 3-D wave fields and show some characteristic differences between purely elastic and viscoelastic and nonlinear wave propagation. The nonlinear propagation is only important when amplitudes are high, such as in the near source region.

0.2 Summary

In this chapter I have described the design and implementation of a modeling tool box mathematically and algorithmically. My goal is to have a portable rapid prototyping environment for new modeling and imaging algorithms that can be designed for any dimension and with a variety of underlying mathematical equations. I succeeded in implementing basic building blocks and algorithms in the Ratfor90 (Ratfor + Fortran90, HPF) programming language. I chose this language beacuse of the compute-intensive nature of seismic wave propagation in realistic complex earth models. I hope that in the future this numerical tool box will be converted to an object-oriented frame work such as C++ and achieve the same performance level. In the demonstrated modeling algorithms I use primarily finite-difference approximations for partial derivative calculation. The Marmousi velocity and density model is a data set and subsurface model designed to test acoustic imaging and velocity estimation algorithms. I use that original model and create a new "elastic" subsurface model assuming a given Poisson's ratio. Modeling wave propagation acoustically and elastically using identical algorithms reveals differences in the recorded wave field that are due to energy conversions caused by elastic propagation. Thus, the acoustically modeled Marmousi dataset is a good test data set for algorithms that were created under the assumption of pure acoustic propagation. However, wave propagation in the real earth is more complicated and acoustic algorithms would experience more difficulties when dealing with more realistic, elastically-modeled seismic data.

Since true amplitude modeling is important for material parameter estimation, it is important to confirm how closely the numerical amplitude behavior agrees with the analytical prediction. I show an example where the reflection response from a single interface agrees well with the analytical Zoeppritz plane wave reflection coefficients. Obviously, if the numerical grid is made very small compared to the wave length of the scattering medium, the finite-difference algorithm will reproduce analytical behavior well. The problem lies in trying to maximize the coarseness of the computational grid so as to minimize computation time and computational resources, but to still get an accurate solution to the problem at hand. Many factors come into play when one tries to achieve this goal. I try to solve one of them by splitting the wave operator using the chain rule of derivatives and implementing a medium and wave field adaptive derivative. I can thus model wave propagation with an optimal derivative operator for both the wave field and the medium parameters.

When one models wave propagation in the near field of seismic sources, the normal linear wave equation fails to adequately describe the wave propagation effects. I use the well known finite-stress-strain description to augment the infinitesimal, linear

elastic wave equation to regimes of finite stresses and strains using modifications of the usual linear derivative operator. The advantage of this approach is that it does not require an estimation of new material parameters. In a second approach I use the one-dimensional Duffing equation and create an anisotropic, three-component, three-dimensional nonlinear wave equation. The Duffing equation is often used to demonstrate chaotic behavior of a physical system when it is periodically driven. Therefore such an extension might be well suited to a seismic vibrator source. Nonetheless, I use the same equation for impulsive sources and show characteristic differences in wave fields produced by propagating in a purely elastic, visco-elastic, and nonlinear homogeneous medium.

The application of the wave propagation tool box to a variety of problems confirms the versatility that this frame work offers for turning mathematical concepts into numerical algorithms. Easy design, implementation and prototyping are possible through the use of a general object-oriented approach.